

# Unearthing the soil carbon food web with high resolution DNA-SIP

Ashley N Campbell and Charles Pepe-Ranney \* † ‡, Chantal Koechli, Sean Berthrong, and Daniel H Buckley ‡

\* These authors contributed equally to the manuscript and should be considered co-first authors, † Department of Microbiology, Cornell University, New York, USA, and ‡ Department of Crop and Soil Sciences, Cornell University, New York, USA

Submitted to Proceedings of the National Academy of Sciences of the United States of America

## Abstract

We identify microorganisms participating in the transformation of xylose or cellulose in soil microcosms by using nucleic acid stable isotope probing (SIP) coupled to next generation sequencing. Microcosms were incubated with  $^{13}\text{C}$ -xylose or  $^{13}\text{C}$ -cellulose and microcosm DNA was interrogated for  $^{13}\text{C}$ -incorporation at days 1, 3, 7, 14 and 30. A total of 49 and 63 unique OTUs assimilated  $^{13}\text{C}$  from xylose and cellulose into DNA, respectively. Incorporation of  $^{13}\text{C}$  from xylose into microcosm DNA was observed at days 1, 3, and 7, while incorporation of  $^{13}\text{C}$  from cellulose peaked at day 14 and was maintained at day 30. Importantly, many cellulose degraders identified in this study are members of cosmopolitan but physiologically uncharacterized soil microbial lineages including *Sphingobacteriia*, *Chloroflexi* and *Planctomycetes*.  $^{13}\text{C}$ -xylose additions precipitated a temporal cascade of  $^{13}\text{C}$ -incorporation activity that could be due to significant predatory interactions among bacteria yet intra-bacteria predatory interactions are rarely considered in soil C cycling conceptual models. Microorganisms that assimilated  $^{13}\text{C}$ -xylose were faster growing and displayed less substrate specificity than microorganisms that incorporated  $^{13}\text{C}$  from cellulose as assessed by predicted *rrn* gene copy number for each OTU and OTU DNA buoyant density shifts in response to  $^{13}\text{C}$ -labeling. Also, microorganisms that assimilated  $^{13}\text{C}$  from xylose were phylogenetically overdispersed whereas  $^{13}\text{C}$ -cellulose assimilating microorganisms were phylogenetically constrained. Describing the ecology and identities of soil C cycling microorganisms will calibrate and inform predictions of terrestrial carbon flux in response to climate change and land management. Tuning terrestrial C flux models with appropriate parameters for soil biomass is crucial for reconciling contrasting predictions of soil as a future C sink and source.

monolayer | structure | x-ray reflectivity | molecular electronics

Abbreviations: SAM, self-assembled monolayer; OTS, octadecyl-  
50 trichlorosilane

## Significance

We have limited understanding of soil carbon (C) cycling yet soil contains a large fraction of the global C pool. Microorganisms mediate most soil C cycling but have proven difficult to study due to the complexity of soil C biochemistry and the wide range of soil microorganisms participating in C reactions. We demonstrate C use dynamics by soil microbial taxa. Furthermore, we identified novel microorganisms involved in cellulose decomposition, the most globally abundant biopolymer. Further application of the method demonstrated in this paper will identify microbial taxa that mediate soil C transformations for more substrates and soils and increase our understanding of global soil C cycling.

## Introduction

Excluding plant biomass, there are 2,300 Pg of carbon (C) stored in soils worldwide which accounts for ~80% of the global terrestrial C pool [1, 2]. When organic C from plants reaches soil it is degraded by fungi, archaea, and bacteria. The majority of plant biomass C in soil is respired and produces 10 times more CO<sub>2</sub> annually than anthropogenic emissions [3]. Global changes in atmospheric CO<sub>2</sub>, temperature, and ecosystem nitrogen inputs are expected to impact soil C input [4]. Current climate change models concur on atmospheric and oceanic but not terrestrial C predictions [5]. Contrasting terrestrial C model predictions reflect how little is known about soil C cycling. Inconsis-

## Reserved for Publication Footnotes

tencies in terrestrial modeling could be improved by elucidating the relationship between dissolved organic C and soil microbial community composition [6].

To establish the relationship between community structure and soil function we must identify the *in situ* activity of specific soil microbes [7]. An estimated 80–90% of soil C cycling is mediated by microorganisms [8, 9] but exploring soil C processing is challenging due to soil’s heterogeneous nature. The majority of microorganisms resist cultivation in the laboratory. Stable-isotope probing (SIP) links genetic identity and activity without cultivation and has been used to expand our knowledge of microbial contributions to biogeochemical processes [10]. Successful applications of SIP have identified organisms which mediate processes performed by a narrow set of functional guilds such as methanogens [11] but SIP has been less applicable in soil C cycling studies due to limitations in resolving power as a result of simultaneous labeling of many different organisms. High throughput DNA sequencing technology, however, has enabled exploration of complex soil C-cycling patterns via SIP.

A temporal activity cascade occurs in natural microbial communities during plant biomass degradation in which labile C is degraded before polymeric C [12, 13]. This study’s aim was to observe C assimilation dynamics in the soil microbial community. Our experimental approach included the addition of a soil organic matter (SOM) simulant to soil microcosms where a single C component was substituted for its  $^{13}\text{C}$  equivalent. Parallel incubations of soils amended with this C mixture allowed us to observe how different C substrates move through the soil microbial community. In this study we used  $^{13}\text{C}$ -xylose and  $^{13}\text{C}$ -cellulose as a proxy for labile and polymeric C, respectively, and coupled nucleic acid SIP with high throughput DNA sequencing. Amplicon sequencing of 16S rRNA genes from gradient fractions of multiple density gradients made it possible to track C assimilation by hundreds of soil taxa.

## Results

We observed C use dynamics in an agricultural soil microbial community by conducting a nucleic acid SIP experiment wherein xylose or cellulose carried the isotopic label. We set up three soil microcosm series (Figure XX). Each microcosm was amended with a C substrate mixture that included cellulose and xylose. The C substrate mixture approximated the C composition of fresh plant biomass. The same mixture was added to all microcosms, however, for each series except the control, xylose or cellulose was substituted for its  $^{13}\text{C}$

counterpart. Microcosms are identified in figures by the following code: “13CXPS” refers to the amendment with  $^{13}\text{C}$ -xylose ( **$^{13}\text{C}$  Xylose Plant Simulant**), “13CCPS” refers to the  $^{13}\text{C}$ -cellulose amendment and “12CCPS” refers to the amendment that only contained  $^{12}\text{C}$  (i.e. control). 5.3 mg C substrate mixture per gram of soil was added to each microcosm representing 18% of the soil C. The mixture included 0.42 mg xylose-C and 0.88 mg cellulose-C per gram soil. Microcosms were harvested at days 1, 3, 7, 14 and 30 during a 30 day incubation.  $^{13}\text{C}$ -xylose assimilation peaked immediately and tapered over the 30 day incubation whereas  $^{13}\text{C}$ -cellulose assimilation peaked two weeks after amendment additions (Figure 1, Figure S1). See Supplemental Note XX for sequencing and density fractionation statistics.

**Soil microcosm microbial community changes with time.** Changes in the bulk soil microcosm microbial community structure and membership correlated significantly with time (Figure S2, p-value 0.23,  $R^2$  0.63, Adonis test [14]). The identity of the  $^{13}\text{C}$ -labeled substrate added to the microcosms did not significantly correlate with bulk soil community structure and membership (p-value 0.35). Additionally, microcosm beta diversity was significantly less than gradient fraction beta diversity (Figure S2, p-value 0.003, “betadisper” function R Vegan package [15, 16]). Twenty-nine OTUs significantly changed in relative abundance with time (“BH” adjusted p-value <0.10, [17]) and of these 29 OTUs, 14 were found to incorporate  $^{13}\text{C}$  from labeled substrates into biomass (Figure S3). Four classes significantly (adjusted P-value <0.10) changed in abundance: *Bacilli* (decreased), *Flavobacteria* (decreased), *Gammaproteobacteria* (decreased) and *Herpetosiphonales* (increased) (Figure S4). Abundances grouped at phylum level for OTUs that incorporated  $^{13}\text{C}$  from cellulose increased with time whereas abundances grouped at the phylum level of OTUs that incorporated  $^{13}\text{C}$  from xylose decreased over time although *Proteobacteria* abundance spiked at day 14 (Figure S5).

**OTUs that assimilated  $^{13}\text{C}$  into DNA.** Within the first 7 days of incubation 63% of  $^{13}\text{C}$ -xylose was respired and only 6% more was respired from day 7 to 30. At day 30, 30% of the  $^{13}\text{C}$  from xylose remained in the soil. An average 16% of the  $^{13}\text{C}$ -cellulose added was respired within the first 7 days, 38% by day 14, and 60% by day 30.

We refer to OTUs that putatively incorporated  $^{13}\text{C}$  into DNA originally from an isotopically labeled substrate as substrate “responders” (see Supplemental Note XX for operational “response” criteria). There were X, X, X, X, and X  $^{13}\text{C}$ -xylose

responders at days 1, 3, 7, 14, 30, respectively (Figure S1). The numerically dominant  $^{13}\text{C}$ -xylose responder phylum shifted from *Firmicutes* to *Bacteroidetes* and then to *Actinobacteria* across days 1, 3 and 7 (Figure 2, Figure 3). *Proteobacteria*  $^{13}\text{C}$ -xylose responders were found at days 1, 3, 7 but peaked at day 7 (Figure 3).

Only 2 and 5 OTUs had incorporated  $^{13}\text{C}$  from  $^{13}\text{C}$ -cellulose at days 3 and 7, respectively. At days 14 and 30, 42 and 39 OTUs incorporated  $^{13}\text{C}$  from  $^{13}\text{C}$ -cellulose into biomass (Figure S1). *Proteobacteria*, *Verrucomicrobia*, and *Chloroflexi* had relatively high numbers of responders with strong response across multiple time points (Figure 2). *Verrucomicrobia*  $^{13}\text{C}$ -cellulose responders were XX% *Spartobacteria*. *Chloroflexi* responders were annotated belonging to the *Herpetosiphonales* and XX. *Cellvibrio* a canonical soil cellulose degrader was found to respond strongly in the microcosms to  $^{13}\text{C}$ -cellulose. See Supplemental Note XX for further analysis of  $^{13}\text{C}$ -responsive OTUs at greater taxonomic resolution.

**Ecological strategies of  $^{13}\text{C}$  responders.**  $^{13}\text{C}$ -xylose responders are generally more abundant members based on relative abundance in bulk DNA SSU rRNA gene content than  $^{13}\text{C}$ -cellulose responders (Figure 4, p-value 0.00028, Wilcoxon Rank Sum test). However, both abundant and rare OTUs responded to  $^{13}\text{C}$ -xylose and  $^{13}\text{C}$ -cellulose (Figure 4). Two  $^{13}\text{C}$ -cellulose responders were not found in any bulk samples (“OTU.862” and “OTU.1312”, Table S1). Of the 10 most abundant responders, 8 are  $^{13}\text{C}$ -xylose responders and 6 of these 8 are consistently among the 10 most abundant OTUs in bulk samples.

Cellulose responders exhibited a greater shift in buoyant density (BD) than xylose responders in response to isotope incorporation (Figure S6, Figure 4, p-value  $1.8610 \times 10^{-6}$ , Wilcoxon Rank Sum test).  $^{13}\text{C}$ -cellulose responders shifted on average  $0.0163 \text{ g mL}^{-1}$  (sd 0.0094) whereas xylose responders shifted on average  $0.0097 \text{ g mL}^{-1}$  (sd 0.0094). For reference, 100%  $^{13}\text{C}$  DNA BD is  $0.04 \text{ g mL}^{-1}$  greater than the BD of its  $^{12}\text{C}$  counterpart. DNA BD increases as its ratio of  $^{13}\text{C}$  to  $^{12}\text{C}$  increases. An organism that only assimilates C into DNA from a  $^{13}\text{C}$  isotopically labeled source, will have a greater  $^{13}\text{C}$ : $^{12}\text{C}$  ratio in its DNA than an organism utilizing a mixture of isotopically labeled and unlabeled C sources (see Supplemental Note XX). We predicted the *rrn* gene copy number for each OTU as described previously CITE.  $^{13}\text{C}$ -xylose responder estimated *rrn* gene copy number was inversely related time of first response (p-value  $2.02 \times 10^{-15}$ , Figure S7). OTUs that first respond at later time

points have fewer estimated *rrn* copy number than OTUs that first respond earlier (Figure S7).

We assessed phylogenetic clustering of  $^{13}\text{C}$ -responsive OTUs with the Nearest Taxon Index (NTI) and the Net Relatedness Index (NRI). Briefly, positive NRI and NTI with corresponding low P-values indicates deep phylogenetic clustering whereas negative NRI with high P-values indicates taxa are overdispersed against the null model CITE. NRI and P-values for substrate responder groups suggest  $^{13}\text{C}$ -xylose responders are overdispersed (NRI: -1.33, P: 0.90) while cellulose responders are clustered (NRI: 4.49, P: 0.001). Nearest taxon indices (NTI) show that both  $^{13}\text{C}$ -cellulose and  $^{13}\text{C}$ -xylose responders are clustered near the tips of the tree (NTI: 1.43 (P: 0.072), 2.69 (P: 0.001), respectively).

## Discussion

**Microbial response to isotopic labels.** DNA-SIP can characterize functional roles for thousands of phylotypes in a single experiment without cultivation. We identified 104 agricultural soil OTUs soil that incorporated  $^{13}\text{C}$  from xylose and/or cellulose into biomass and characterized substrate specificity and C-cycling dynamics for these OTUs. We propose C added to soil microcosms took the following path through the microbial food web (Figure S8): fast-growing *Firmicutes* spore formers first assimilated labile C followed by *Bacteroidetes*, *Actinobacteria* and *Proteobacteria* phylotypes. The *Bacteroidetes*, *Actinobacteria* and *Proteobacteria* phylotypes may have also preyed on the rapidly responding *Firmicutes*. Bacteria incorporated C from cellulose into biomass after 14 days. Canonical cellulose degrading bacteria such as *Cellvibrio* and members of cosmopolitan yet functionally uncharacterized soil phylogenetic groups like *Chloroflexi*, *Planctomycetes* and *Verrucomicrobia*, specifically the *Spartobacteria*, decomposed cellulose.

**Ecological strategies of soil microorganisms participating in the decomposition of organic matter.** We assessed  $^{13}\text{C}$ -responsive OTU ecological strategy by estimating each OTU's *rrn* gene copy number and the BD shift upon  $^{13}\text{C}$ -labeling. *rrn* gene copy number correlates positively with growth rate [18] and BD shift is indicative of substrate specificity (see results).  $^{13}\text{C}$ -cellulose responsive OTUs grow slower (Figure 4, Figure S7), have greater substrate specificity (Figure 4), and are generally lower abundance members of the bulk community than  $^{13}\text{C}$ -xylose responsive OTUs (Figure 4). The high abundance of xylose responders may also be due in part to high *rrn* gene copy number.  $^{13}\text{C}$ -xylose responsive OTUs that incorporate  $^{13}\text{C}$  into

biomass at day one had greater *rrn* gene copy number than OTUs that responded later to  $^{13}\text{C}$ -xylose (Figure 4, Figure S7) suggesting fast-growing microbes assimilated  $^{13}\text{C}$  from xylose before slow growers.

NRI values quantify phylogenetic clustering [19] and have been used to assess clustering of soil OTUs that responded similarly to soil wet up [20, 21]. To our knowledge assessing the phylogenetic clustering of OTUs found to incorporate heavy isotopes into biomass during SIP incubations has not been attempted. We found that cellulose and xylose responders are clustered and overdispersed, respectively. This suggests that the ability to degrade cellulose is phylogenetically conserved possibly reflecting the complexity of cellulose degradation biochemistry. The positive relationship with a physiological trait’s phylogenetic depth and complexity has been noted previously [22] and the  $^{13}\text{C}$ -cellulose response trait depth observed in this study (X.XX 16S rRNA gene sequence divergence) is on the same order as that observed for glycoside hydrolases which are diagnostic enzymes in cellulose degradation [23]. Overdispersion, as we saw for the  $^{13}\text{C}$ -xylose responsive OTUs, may be indicative of an readily horizontally transferred trait and/or a trait that is broadly distributed phylogenetically. It’s not clear, though, if all  $^{13}\text{C}$ -xylose responsive organisms were labeled as a result of primary xylose assimilation (see below), and therefore it’s not clear if  $^{13}\text{C}$ -xylose responsive OTUs in this experiment constitute a single ecologically meaningful group or multiple ecological groups. TALK ABOUT PHLO COHERENT TEMPORAL RESPONSE.

Intuitively we infer C cycling functional guild diversity from the distribution of diagnostic genes in genomes or from screen culture collections for the trait in question CITE. For instance, the wide distribution of the glycolysis operon is interpreted as evidence that many soil microorganisms participate in glucose turnover CITE. *in situ* functional guild diversity, however, can vary significantly from diversity assessed by functionally screening isolates and/or genomes. Xylose use in soil, for instance, may be less a function of catabolic pathway distribution among genomes and more a function of lifestyle. Soil is characterized by pulse delivery of nutrients and resources that coincide with phenomena including seasonal change CITE, land management CITE, and rainfall CITE. Therefore, rapid growth rates and/or the rapid resuscitation upon wet up may control labile soil C assimilation. Growth rate and dessication resistance are phylogenetically conserved unlike labile C degradation CITE so labile C assimilation may be deceptively conserved as well. DNA-SIP is useful for establishing *in situ* phylogenetic clustering and diversity

of functional guilds because DNA-SIP can incorporate life history strategies into trait functional guild identification by targeting active microorganisms. Snapshot estimates of community composition inform soil structure function studies CITE Fierer but labile C decomposition might not be linked to snapshot community structure but rather to community structure dynamics. Fast growing spore formers, for example, would not need to maintain high abundance to significantly mediate cycling of pulse delivered resources. This accentuates the usefulness of DNA-SIP for describing soil ecology as DNA-SIP assesses the activity of microorganisms.

Need to incorporate Fierer 2007 paper

Paenibacillus Neufeld

Thompson “all bands enriched”

**Implications for soil C cycling models.** Land management, climate, pollution and disturbance can influence soil community composition [24] which in turn influences soil biogeochemical process rates (e.g. [25]). Assessing functional group diversity and establishing identities of functional group members is necessary to predict how biogeochemical process rates will change with community composition [24, 26]. Aggregate biogeochemical processes that are the sum of many subprocesses such as soil respiration involve a broad array of taxa and are assumed to be less influenced by community change than narrow processes that involve a single, specific chemical transformation by a smaller suite of microbial participants [26]. Within an aggregate process such as decomposition, subprocesses can be further classified as broad or narrow [24]. Labile and recalcitrant C decomposition are considered to be carried out by “broad” and “narrow” functional guilds, respectively [24]. However, the diversity of active labile C and insoluble, polymeric C decomposers in soil has not been directly quantified. Notably, we found more OTUs responded to  $^{13}\text{C}$ -cellulose, 63, than  $^{13}\text{C}$ -xylose, 49. Also, it is possible that many  $^{13}\text{C}$ -xylose responders are predatory bacteria as opposed to primary labile C degraders (see below). Cellulose and xylose decomposer functional guilds were non-overlapping in membership – of 104  $^{13}\text{C}$ -responders only 8 responded to both cellulose and xylose – and represented a small fraction of total soil community diversity (Figure 5). While xylose use is undoubtedly more widely distributed among global microorganisms than the ability to degrade cellulose, the number of active xylose utilizers in our microcosms was not greater than the number of cellulose decomposers.

Both  $^{13}\text{C}$ -cellulose and  $^{13}\text{C}$ -xylose responders largely clustered near the tips of the phylogenetic tree ( $\text{NTI} > 0$ ) at taxonomic levels broader

than the OTUs established in this study (Figure S9). Therefore  $^{13}\text{C}$ -responders distribute into fewer clades than OTUs (Figure S9).  $^{13}\text{C}$ -xylose responders formed clades at depth of X.XX sequence divergence (consenTrait) while our OTUs were established at 0.03 sequence divergence. Active cellulose and xylose responder groups were “narrow” in that few lineages relative to total observed lineages were active participants in cellulose or xylose decomposition but there is no quantitative definition of what constitutes “narrow” versus “broad” in the literature. HGT SENTENCE. TALK ABOUT TRESEDER NUMBERS?

The activity succession from *Firmicutes* to *Bacteroidetes* and finally *Actinobacteria* in response to  $^{13}\text{C}$ -xylose addition is a trophic cascade and/or the manifestation functional groups tuned to different resource concentrations. *Actinobacteria* (e.g. *Agromyces*) and *Bacteroidetes* have been previously implicated as predatory soil bacteria [27, 28], however, and the activity peak of *Bacteroidetes* and *Actinobacteria* occurred with a corresponding decrease in *Firmicutes*  $^{13}\text{C}$ -xylose responder relative abundance. Considering that *Agromyces* and certain *Bacteroidetes* types are likely soil predators one parsimonious hypothesis for the  $^{13}\text{C}$ -labelling of *Bacteroidetes* and *Actinobacteria* with a corresponding decrease in abundance of  $^{13}\text{C}$ -labeled *Firmicutes* is that the *Bacteroidetes* and *Actinobacteria* fed on  $^{13}\text{C}$ -labeled *Firmicutes*. If the temporal dynamics of  $^{13}\text{C}$ -xylose incorporation are due to trophic interactions, many, if not most, fast-growing labile C degraders were consumed by predatory bacteria. Hence, predatory interactions between soil bacteria may be of importance for modelling soil C turnover yet intra-bacteria trophic interactions in soil C cycling models are rarely considered (e.g. [29]).

We propose two scenarios in the context of our results wherein C dynamics and fate would be affected by community composition. Genomic evidence shows cellulose degradation is a phylogenetically conserved trait CITE Allison. Our study is the first to evaluate the phylogenetic conservation of soil cellulose degradation *in situ* via DNA-SIP and our results are consistent with genomic evidence. Decreasing cellulose degraders would diminish cellulose decomposition process rates as few soil microorganisms can fill the phylogenetically conserved cellulose degradation niche. Ecosystem function could be renewed by dispersed cellulose decomposers, however. For labile C decomposition, the absence fast growing spore formers would enable other microbes to assimilate labile C provided dispersal does not enable rapid recolonization CITE. Primary labile C degraders in this study grow fast, and form spores. These distinct ecological strategies might indicate distinct C use

dynamics and/or resource allocation. New labile C degraders may metabolize and allocate labile C differently thus changing labile C dynamics and fate. Further, labile C degrader substitution could affect biomass C turnover by predatory bacteria that feed on fast growing, spore forming labile C decomposers. On the other hand, spore formation enables dispersal which would allow fast growing spore formers to continuously occupy the labile C decomposition niche even when washed out of an environment CITE. One proposed mechanism for similar decomposition rates of labile C across soils varying in community composition is that labile C can be used widely by microorganisms CITE. An alternative hypothesis for consistent labile C process rates across different soils is that labile C degraders are easily dispersed. Notably, other lineages implicated in rapid labile C turnover include members of the *Actinobacteria* CITE Placella and many soil *Actinobacteria* form hyphae that facilitate dispersal CITE. The two hypotheses are not mutually exclusive, but our results suggest that environmental conditions unfavorable to fast-growing spore-formers and/or quickly resuscitated, hyphal *Actinobacteria* CITE may impact labile C dynamics and fate.

**Conclusion.** Microorganisms sequester atmospheric C and respire SOM influencing climate change on a global scale but we do not know which microorganisms carry out specific soil C transformations. In this experiment microbes from physiologically uncharacterized but ubiquitous soil lineages participated in cellulose decomposition. Cellulose C degraders included members of the *Verrucomicrobia* (*Spartobacteria*), *Chloroflexi*, *Bacteroidetes* and *Planctomycetes*. *Spartobacteria* in particular are globally cosmopolitan soil microorganisms and are often the most abundant *Verrucomicrobia* order in soil [30]. Labile C in our microcosms was assimilated by fast-growing *Firmicutes* spore formers. *Bacteroidetes* and *Actinobacteria* phylotypes previously implicated as predators by have fed on the fast growing *Firmicutes*. Our results suggest that, cosmopolitan *Spartobacteria* may degrade cellulose on a global scale, trophic interactions within bacteria are important for modeling soil C cycling, and functional guild diversity may be constrained by ecological strategies which can be more phylogenetically conserved than catabolic pathways.

## Methods

Additional information on sample collection and analytical methods is provided in SI Materials and Methods.

Twelve soil cores (5 cm diameter x 10 cm depth) were collected from six random sampling locations within an organically managed agricultural field in

Penn Yan, New York. Soils were pretreated by sieving (2 mm), homogenizing sieved soil, and pre-  
 535 incubating 10 g of dry soil weight in flasks for 2 weeks. Soils were amended with a 5.3 mg g soil<sup>-1</sup>  
 carbon mixture; representative of natural concen-  
 595 trations [31]. Mixture contained 38% cellulose,  
 23% lignin, 20% xylose, 3% arabinose, 1% galac-  
 540 tose, 1% glucose, and 0.5% mannose by mass, with  
 the remaining 13.5% mass composed of an amino  
 acid (in-house made replica of Teknova C0705) and  
 basal salt mixture (Murashige and Skoog, Sigma  
 Aldrich M5524). Three parallel treatments were  
 545 performed; (1) unlabeled control, (2)<sup>13</sup>C-cellulose,  
 (3)<sup>13</sup>C-xylose (98 atom% <sup>13</sup>C, Sigma Aldrich).  
 Each treatment had 2 replicates per time point  
 (n = 4) except day 30 which had 4 replicates; total  
 550 microcosms per treatment n = 12, except <sup>13</sup>C-  
 cellulose which was not sampled at day 1, n =  
 10. Other details relating to substrate addition  
 can be found in SI. Microcosms were sampled de-  
 structively (stored at -80°C until nucleic acid pro-  
 555 cessing) at days 1 (control and xylose only), 3, 7,  
 14, and 30.

Nucleic acids were extracted using a modified Griffiths protocol [32]. To prepare nucleic acid extracts for isopycnic centrifugation as previously described [33], DNA was size selected (>4kb) using  
 560 1% low melt agarose gel and β-agarase I enzyme extraction per manufacturers protocol (New England Biolab, M0392S). For each time point in the series isopycnic gradients were setup using a modified protocol [34] for a total of five <sup>12</sup>C-control, five  
 565 <sup>13</sup>C-xylose, and four <sup>13</sup>C-cellulose microcosms. A density gradient (average density 1.69 g mL<sup>-1</sup>) so-  
 lution of 1.762 g cesium chloride (CsCl) mL<sup>-1</sup> in  
 620 gradient buffer solution (pH 8.0 15 mM Tris-HCl,  
 15 mM EDTA, 15 mM KCl) was used to sepa-  
 570 rate <sup>13</sup>C-enriched and <sup>12</sup>C-non-enriched DNA. Each  
 gradient was loaded with approximately 5 µg of  
 625 DNA and ultracentrifuged for 66 h at 55,000 rpm  
 and room temperature (RT). Fractions of ~100 µL  
 were collected from below by displacing the DNA-  
 575 CsCl-gradient buffer solution in the centrifugation  
 tube with water using a syringe pump at a flow  
 rate of 3.3 µL s<sup>-1</sup> [35] into Acroprep<sup>TM</sup> 96 filter  
 plate (Pall Life Sciences 5035). The refractive in-  
 630 dex of each fraction was measured using a Reichart  
 AR200 digital refractometer modified as previously  
 described [33] to measure a volume of 5 µL. Then  
 buoyant density was calculated from the refractive  
 index as previously described [33] (see also SI). The  
 635 collected DNA fractions were purified by repetitive  
 washing of Acroprep filter wells with TE. Finally,  
 50 µL TE was added to each fraction then resus-  
 640 pended DNA was pipetted off the filter into a new  
 microfuge tube.

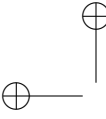
For every gradient, 20 fractions were chosen for  
 590 sequencing between the density range 1.67-1.75 g  
 645

mL<sup>-1</sup>. Barcoded 454 primers were designed using 454-specific adapter B, 10 bp barcodes [36], a 2 bp linker (5'-CA-3'), and 806R primer for reverse primer (BA806R); and 454-specific adapter A, a 2 bp linker (5'-TC-3'), and 515F primer for forward primer (BA515F). Each fraction was PCR amplified using 0.25 µL 5 U µl<sup>-1</sup> AmpliTaq Gold (Life Technologies, Grand Island, NY; N8080243), 2.5 µL 10X Buffer II (100 mM Tris-HCl, pH 8.3, 500 mM KCl), 2.5 µL 25 mM MgCl<sub>2</sub>, 4 µL 5 mM dNTP, 1.25 µL 10 mg mL<sup>-1</sup> BSA, 0.5 µL 10 µM BA515F, 1 µL 5 µM BA806R, 3 µL H<sub>2</sub>O, 10 µL 1:30 DNA template) in triplicate. Samples were normalized either using Pico green quantification and manual calculation or by SequalPrep<sup>TM</sup> normalization plates (Invitrogen, Carlsbad, CA; A10510), then pooled in equimolar concentrations. Pooled DNA was gel extracted from a 1% agarose gel using Wizard SV gel and PCR clean-up system (Promega, Madison, WI; A9281) per manufacturer's protocol. Amplicons were sequenced on Roche 454 FLX system using titanium chemistry at Selah Genomics (formerly EnGenCore, Columbia, SC)

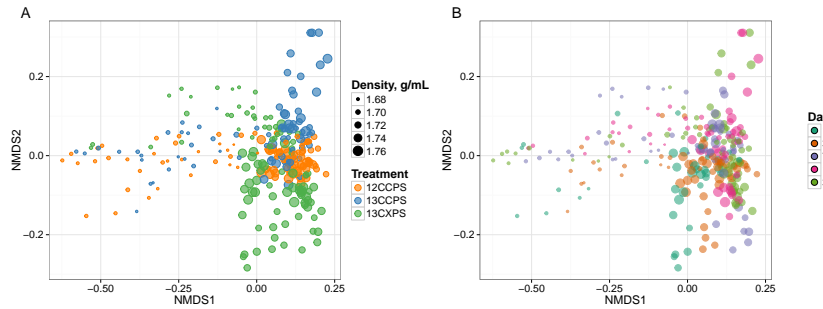
## 615 References

1. Amundson R (2001) The carbon budget in soils. *Annu Rev Earth Planet Sci* 29(1): 535–562.
2. Batjes N-H (1996) Total carbon and nitrogen in the soils of the world. *European Journal of Soil Science* 47(2): 151–163.
3. Chapin F (2002) Principles of terrestrial ecosystem ecology.
4. Groenigen K-J, Graaff M-A, Six J, Harris D, Kuikman P, Kessel C (2006) The impact of elevated atmospheric CO<sub>2</sub> on soil C and N dynamics: a meta-analysis. *Managed Ecosystems and CO<sub>2</sub>* (Springer Science, Berlin Heidelberg), pp 373–391.
5. Friedlingstein P, Cox P, Betts R, Bopp L, von W-B, Brovkin V, et al. (2006) Climate–carbon cycle feedback analysis: Results from the C4 model intercomparison. *J Climate* 19(14): 3337–3353.
6. Neff J-C, Asner G-P (2001) Dissolved organic carbon in terrestrial ecosystems: synthesis and a model. *Ecosystems* 4(1): 29–48.
7. O'Donnell A-G, Seasman M, Macrae A, Waite I, Davies J-T (2002) Plants and fertilisers as drivers of change in microbial community structure and function in soils. *Interactions in the Root Environment: An Integrated Approach* (Springer, Netherlands), pp 135–145.
8. Coleman D-C, Crossley D-A (1996) Fundamentals of Soil Ecology.

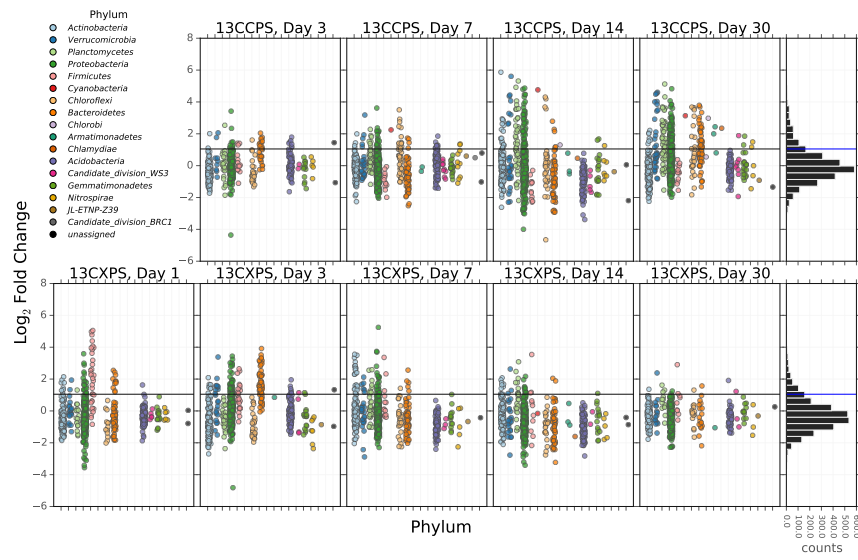
9. Nannipieri P, Ascher J, Ceccherini M-T, Landi L, Pietramellara G, Renella G (2003) Microbial diversity and soil functions. *European Journal of Soil Science* 54(4): 655–670.
10. Chen Y, Murrell J-C (2010) When metagenomics meets stable-isotope probing: progress and perspectives. *Trends Microbiol* 18(4): 157–163.
11. Lu Y (2005) In situ stable isotope probing of methanogenic archaea in the rice rhizosphere. *Science* 309(5737): 1088–1090.
12. Hu S, van Bruggen A-HC (1997) Microbial dynamics associated with multiphasic decomposition of <sup>14</sup>C-Labeled Cellulose in Soil. *Microb Ecol* 33(2): 134–143.
13. Rui J, Peng J, Lu Y (2009) Succession of bacterial populations during plant residue decomposition in rice field soil. *Appl Environ Microbiol* 75(14): 4879–4886.
14. Anderson M-J (2001) A new method for non-parametric multivariate analysis of variance. *Austral Ecology* 26(1): 32–46.
15. Anderson M-J, Ellingsen K-E, McArdle B-H (2006) Multivariate dispersion as a measure of beta diversity. *Ecology Letters* 9(6): 683–693.
16. Oksanen J, Kindt R, Legendre P, OHara B, Stevens M-HH, Oksanen M-J, et al. (2007) The vegan package.
17. Benjamini Y, Hochberg Y (1995) Controlling the false discovery rate: a practical and powerful approach to multiple testing. *Journal of the Royal Statistical Society, Series B* 57(1): 289–300.
18. Klappenbach J, Saxman P, Cole J, Schmidt T (2001) rrndb: the Ribosomal RNA Operon Copy Number Database. *Nucleic Acids Res* 29(1): 181–184.
19. Webb C-O (2000) Exploring the phylogenetic structure of ecological communities: an example for rain forest trees.. *The American Naturalist* 156(2): 145–155.
20. Evans S-E, Wallenstein M-D (2014) Climate change alters ecological strategies of soil bacteria. *Ecol Lett* 17(2): 155–164.
21. Placella S-A, Brodie E-L, Firestone M-K (2012) Rainfall-induced carbon dioxide pulses result from sequential resuscitation of phylogenetically clustered microbial groups. *PNAS* 109(27): 10931–10936.
22. Martiny A-C, Treseder K, Pusch G (2013) Phylogenetic conservatism of functional traits in microorganisms. *ISMEJ* 7(4): 830–838.
23. Berlemont R, Martiny A-C (???) Phylogenetic distribution of potential cellulases in bacteria. *Appl Environ Microbiol* 79(5): 1545–1554.
24. McGuire K-L, Treseder K-K (2010) Microbial communities and their relevance for ecosystem models: Decomposition as a case study. *Soil Biology and Biochemistry* 42(4): 529–535.
25. Berlemont R, Allison S-D, Weihe C, Lu Y, Brodie E-L, Martiny J-BH, et al. (2014) Cellulolytic potential under environmental changes in microbial communities from grassland litter. *Front Microbiol* 5: 639.
26. Schimel J (1995) Ecosystem consequences of microbial diversity and community structure. *Arctic and alpine biodiversity: patterns, causes and ecosystem consequences*, , eds. III P-DFSC, Körner P-DC, Ecological Studies (Springer, Berlin Heidelberg), pp 239–254.
27. Lueders T, Kindler R, Miltner A, Friedrich M-W, Kaestner M (2006) Identification of bacterial micropredators distinctively active in a soil microbial food web. *Appl Environ Microbiol* 72(8): 5342–5348.
28. Casida L-E (1983) Interaction of Agromyces ramosus with Other Bacteria in Soil.. *Appl Environ Microbiol* 46(4): 881–888.
29. Moore J-C, Walter D-E, Hunt H-W (1988) Arthropod Regulation of Micro- and Mesobiota in Below-Ground Detrital Food Webs. *Annu Rev Entomol* 33(1): 419–435.
30. Bergmann G-T, Bates S-T, Eilers K-G, Lauber C-L, Caporaso J-G, Walters W-A, et al. (2011) The under-recognized dominance of Verrucomicrobia in soil bacterial communities. *Soil Biology and Biochemistry* 43(7): 1450–1455.
31. Schneckenberger K, Demin D, Stahr K, Kuzyakov Y (2008) Microbial utilization and mineralization of <sup>14</sup>C glucose added in six orders of concentration to soil. *Soil Biology and Biochemistry* 40(8): 1981–1988.
32. Griffiths R-I, Whiteley A-S, O'Donnell A-G, Bailey M-J (2000) Rapid method for coextraction of DNA and RNA from natural environments for analysis of ribosomal DNA- and rRNA-based microbial community composition. *Appl Environ Microbiol* 66(12): 5488–5491.
33. Buckley D-H, Huangyutitham V, Hsu S-F, Nelson T-A (2007) Stable isotope probing with <sup>15</sup>N achieved by disentangling the effects of genome G+C content and isotope enrichment on dna Density. *Appl Environ Microbiol* 73(10): 3189–3195.
34. Neufeld J-D, Vohra J, Dumont M-G, Lueders T, Manefield M, Friedrich M-W, et al. (2007) DNA stable-isotope probing. *Nature Protocols* 2(4): 860–866.
35. Manefield M, Whiteley A-S, Griffiths R-I, Bailey M-J (2002) RNA Stable isotope probing a novel means of linking microbial community function to phylogeny. *Appl Environ Microbiol* 68(11): 5367–5373.
36. Hamady M, Walker J-J, Harris J-K, Gold N-J, Knight R (2008) Error-correcting barcoded



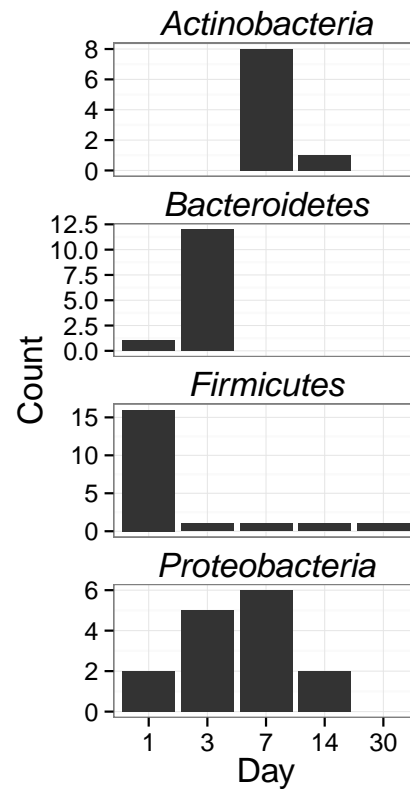
primers for pyrosequencing hundreds of samples in multiplex. *Nat Meth* 5(3): 235–237.



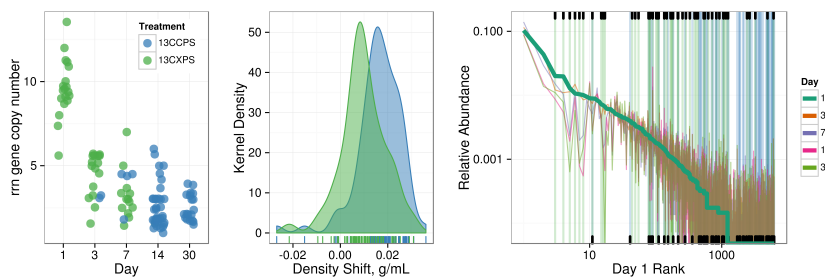
**Fig. 1.** NMDS analysis from weighted unifrac distances of 454 sequence data from SIP fractions of each treatment over time. Twenty fractions from a CsCl gradient fractionation for each treatment at each time point were sequenced (Fig. S1). Each point on the NMDS represents the bacterial composition based on 16S sequencing for a single fraction where the size of the point is representative of the density of that fraction and the colors represent the treatments (A) or days (B).



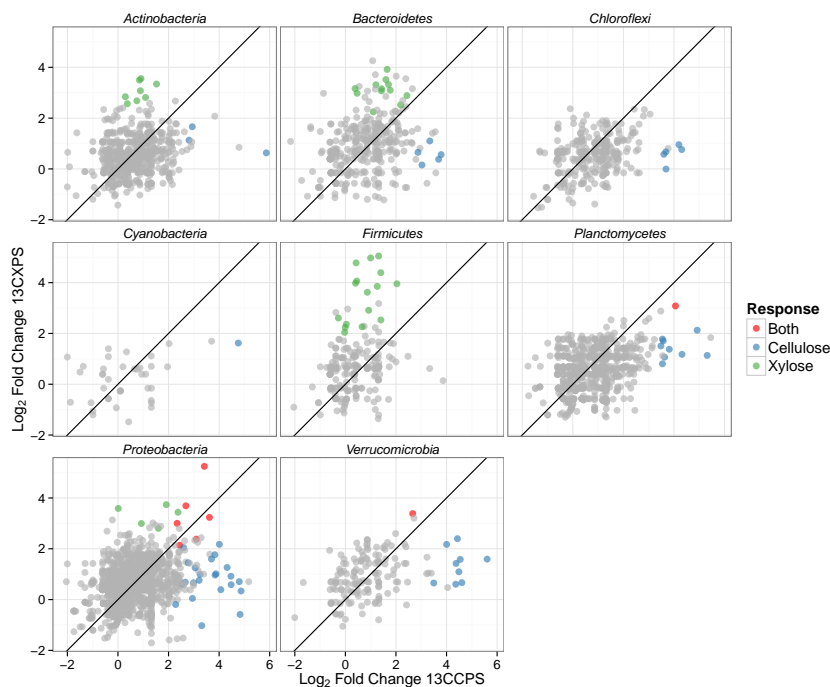
**Fig. 2.** Log<sub>2</sub> fold change of <sup>13</sup>C-responders in cellulose treatment (top) and xylose treatment (bottom). Log<sub>2</sub> fold change is based on the relative abundance in the experimental treatment compared to the control within the density range 1.7125–1.755 g ml<sup>-1</sup>. Taxa are colored by phylum. ‘Counts’ is a histogram of log<sub>2</sub> fold change values.



**Fig. 3.** Counts of  $^{13}\text{C}$ -xylose responders in the *Actinobacteria*, *Bacteroidetes*, *Firmicutes* and *Proteobacteria* at days 1, 3, 7 and 30.

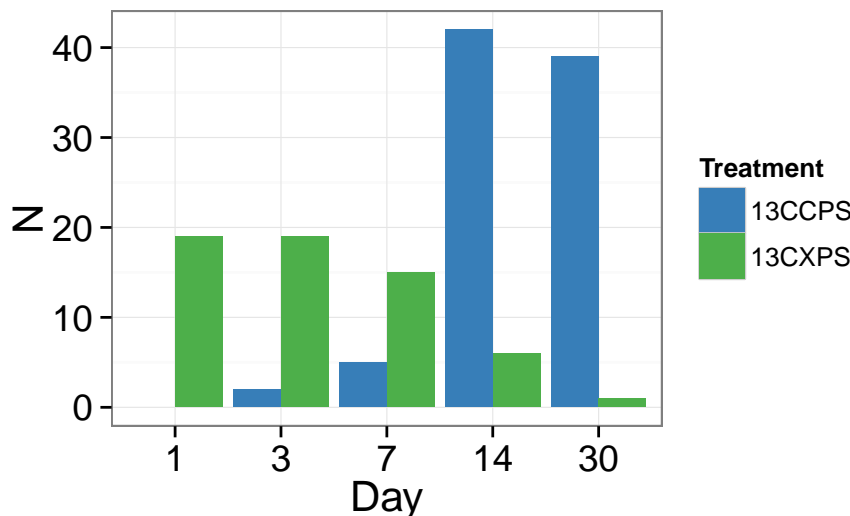


**Fig. 4.**  $^{13}\text{C}$ -responder characteristics based on density shift (A) and rank (B). Kernel density estimation of  $^{13}\text{C}$ -responder's density shift in cellulose treatment (blue) and xylose treatment (green) demonstrates degree of labeling for responders for each respective substrate.  $^{13}\text{C}$ -responders in rank abundance are labeled by substrate (cellulose, blue; xylose, green). Ticks at top indicate location of  $^{13}\text{C}$ -xylose responders in bulk community. Ticks at bottom indicate location of  $^{13}\text{C}$ -cellulose responders in bulk community. OTU rank was assessed from day 1 bulk samples.

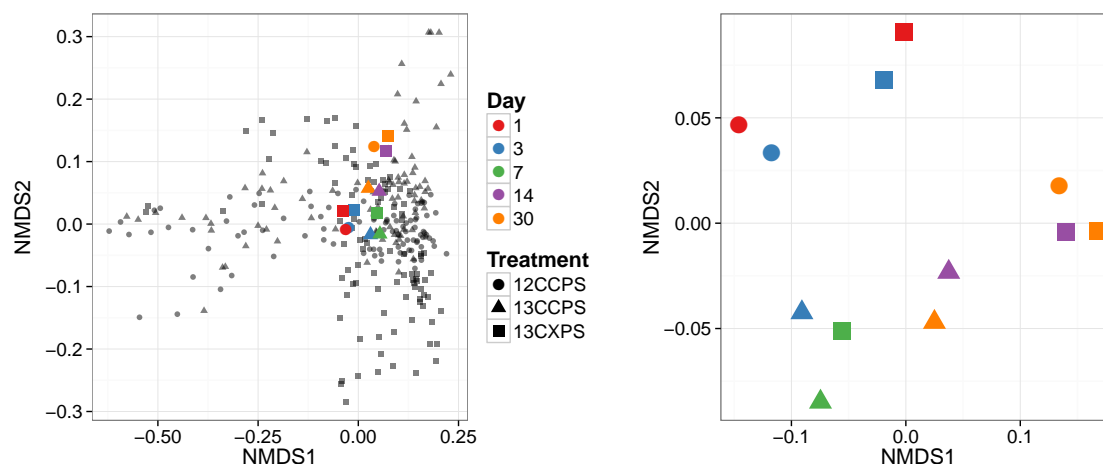


**Fig. 5.** Maximum log<sub>2</sub> fold change in response to labeled substrate incorporation for each substrate and all OTUs that pass sparsity filtering in both substrate analyses. Points colored by response. Line has slope of 1 with intercept at the origin. OTUs falling in the top-right quadrant responded to both substrates while those in the top-left and bottom-right responded to <sup>13</sup>C-xylose and <sup>13</sup>C-cellulose, respectively.

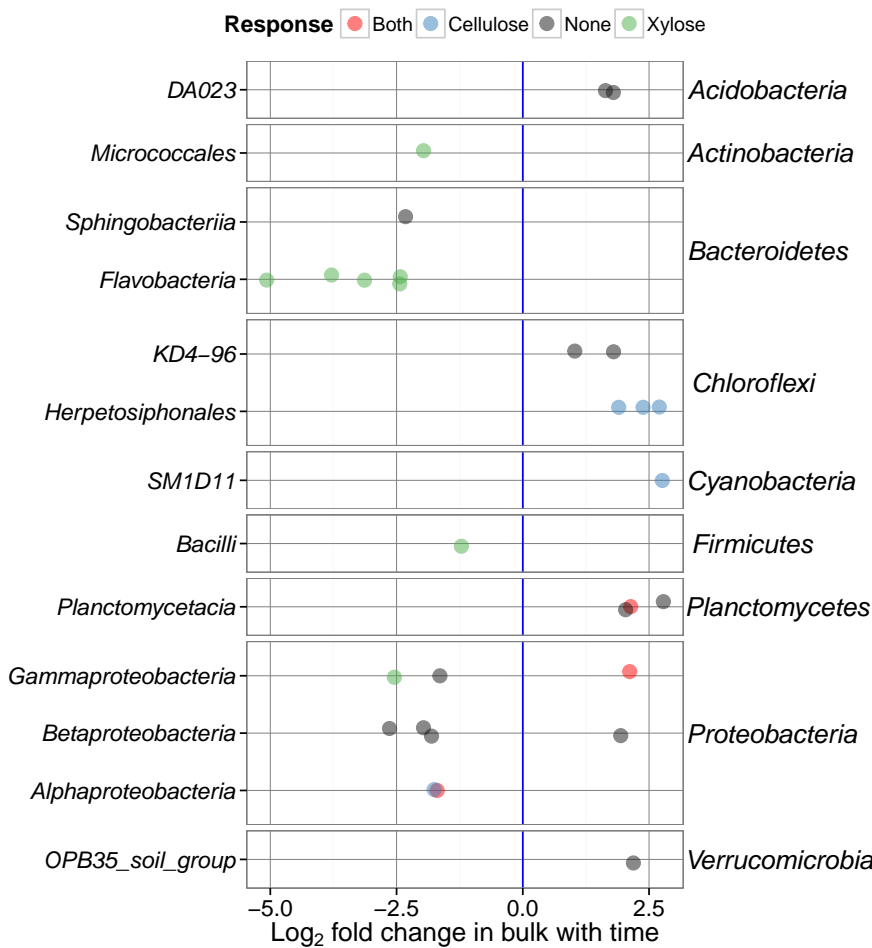
**Supplemental Figures and Tables**



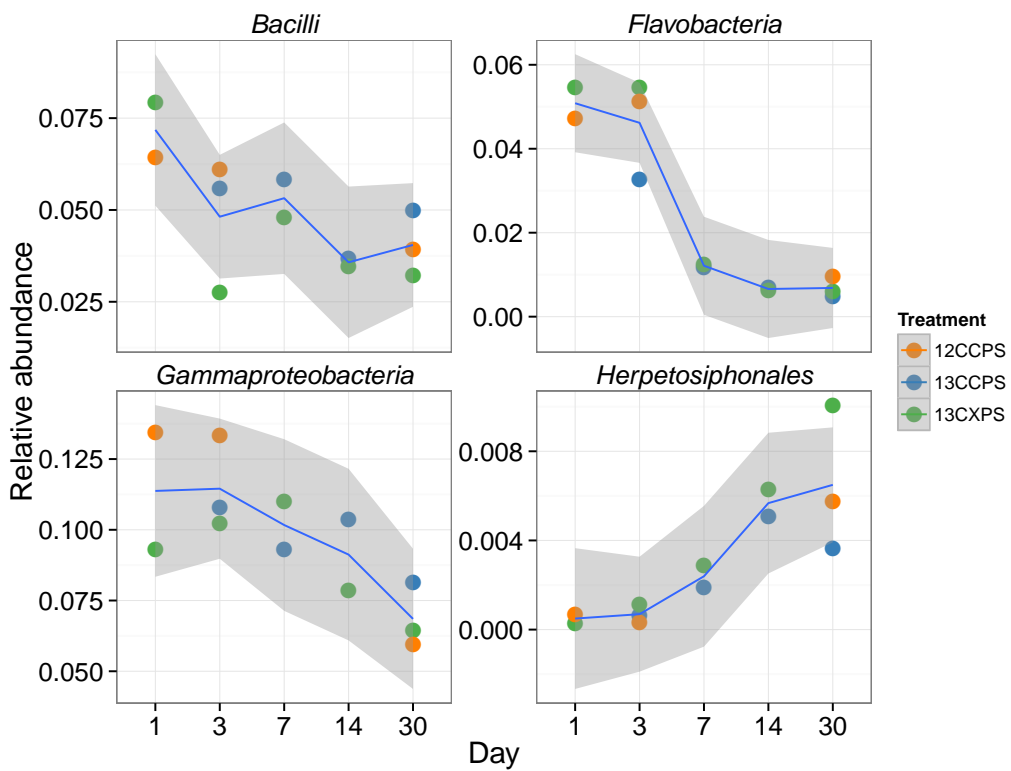
**Fig. S1.** Counts of responders to each isotopically labeled substrate (cellulose and xylose) over time.



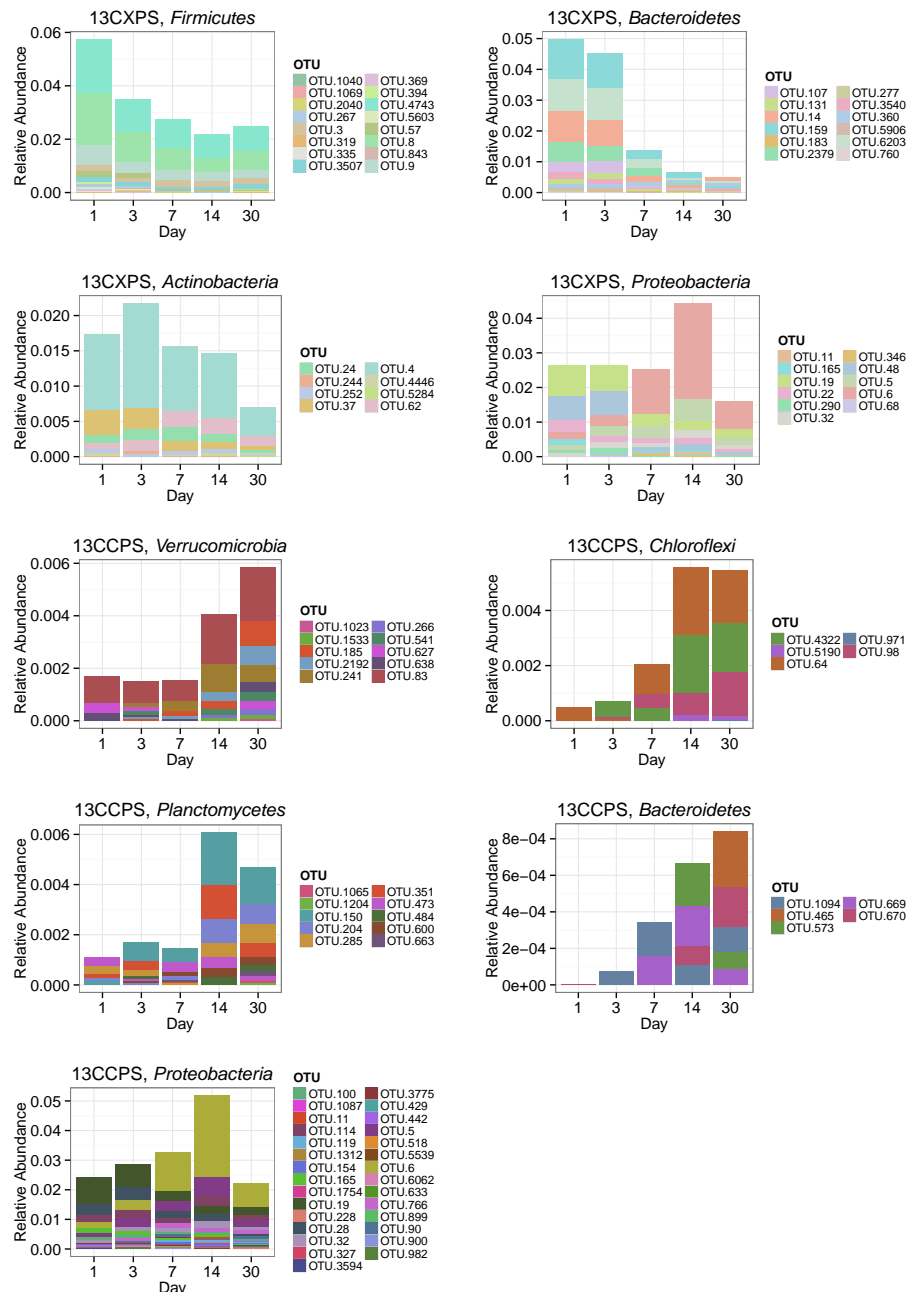
**Fig. S2.** Ordination of bulk gradient fraction phylogenetic profiles.



**Fig. S3.** Fold change  $\text{time}^{-1}$  for OTUs that changed significantly in abundance over time. One panel per phylum (phyla indicated on the right). Taxonomic class indicated on the left.



**Fig. S4.** Relative abundance versus day for classes that changed significantly in relative abundance with time.

**Fig. S5.** Sum of bulk abundances with selected phylum for responder OTUs.

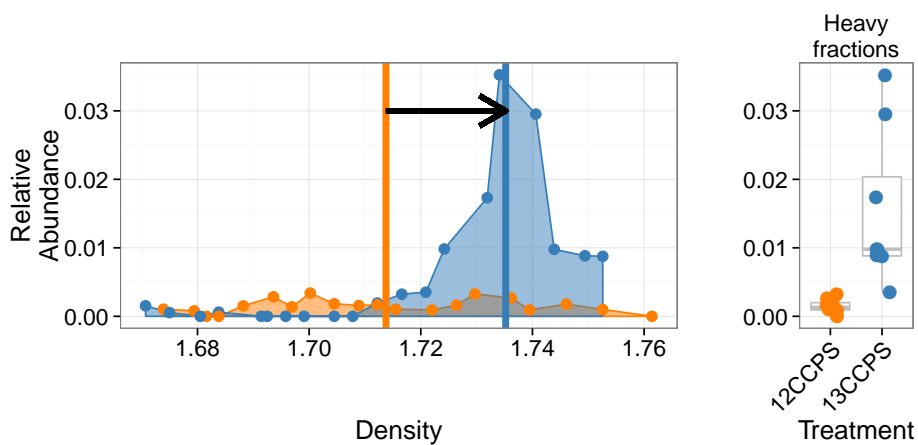


**Fig. S6.** Density profile for a single  $^{13}\text{C}$ -cellulose “responder” OTU in the labeled gradient, blue, and the control gradient, orange. Vertical lines show center of mass for each density profile and arrow denotes the magnitude and direction of the BD shift upon labeling. Panel at right shows relative abundance values in the heavy fractions for each gradient.

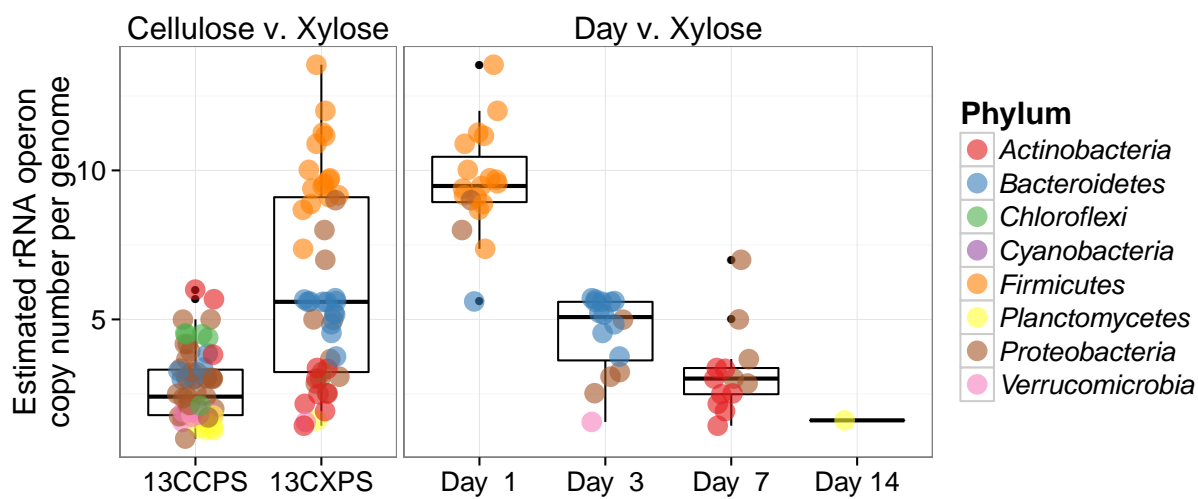


**Fig. S7.** Estimated rRNA operon copy number per genome for  $^{13}\text{C}$  responding OTUs. Panel titles indicate which labeled substrate(s) are depicted.

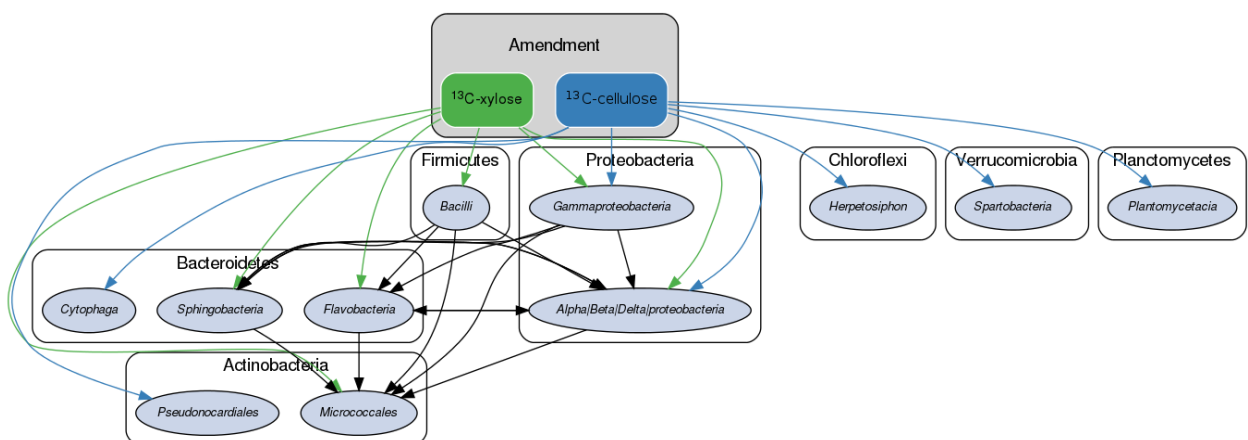


**Fig. S8.** Conceptual model of soil food web in this experiment. Taxa shown possessed at least two <sup>13</sup>C responder OTUs for a given C substrate. *Proteobacteria* response was too varied taxonomically to depict at higher taxonomic resolution in this format. Black arrows indicate possible predator/prey interactions whereas colored arrows represent possible routes of primary degradation (green: xylose, blue: cellulose).

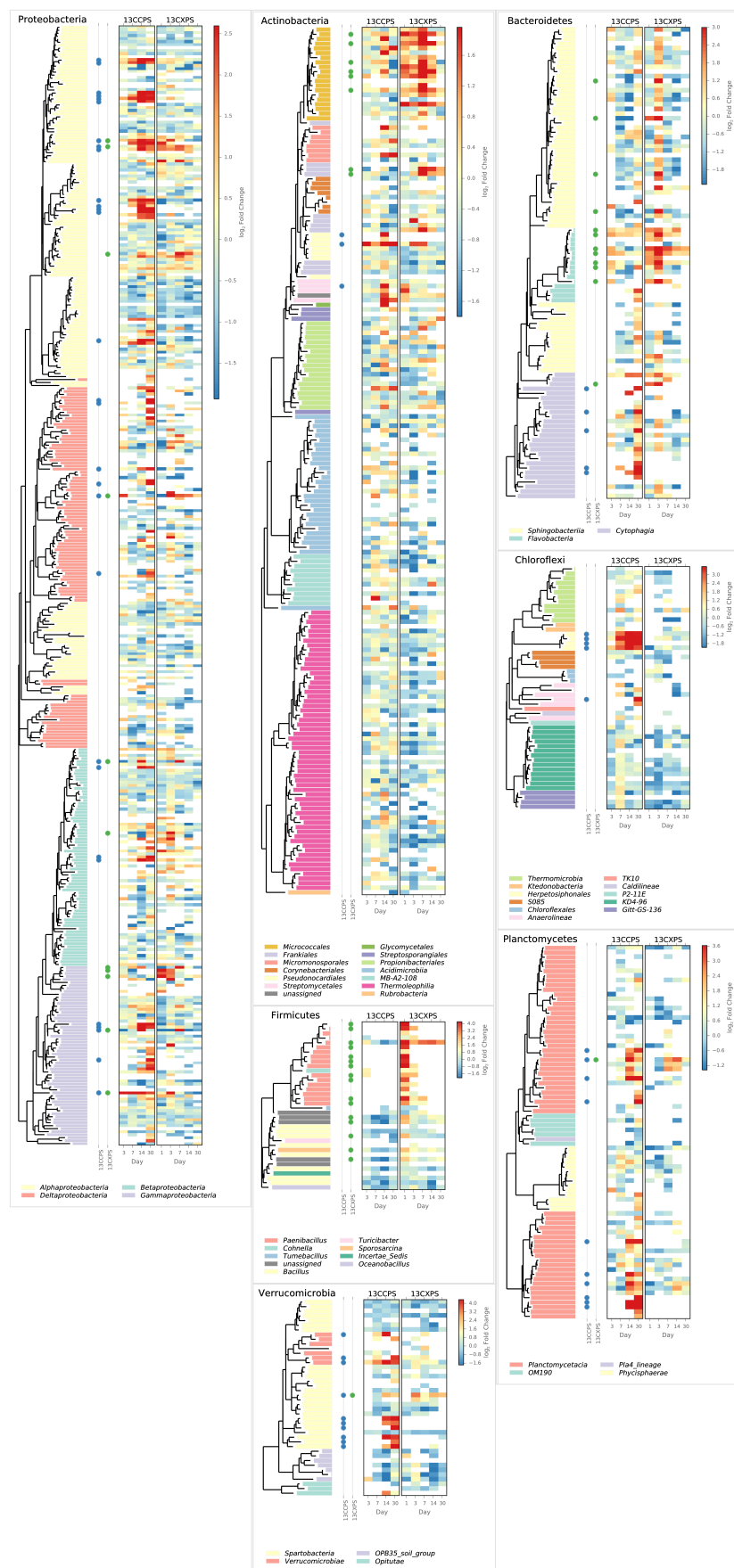


**Fig. S9.** Phylum specific trees. Heatmap indicates fold change between heavy fractions of control gradients versus labeled gradients. Dots indicate the position of “responders” to  $^{13}\text{C}$ -xylose (green) or  $^{13}\text{C}$ -cellulose (blue).

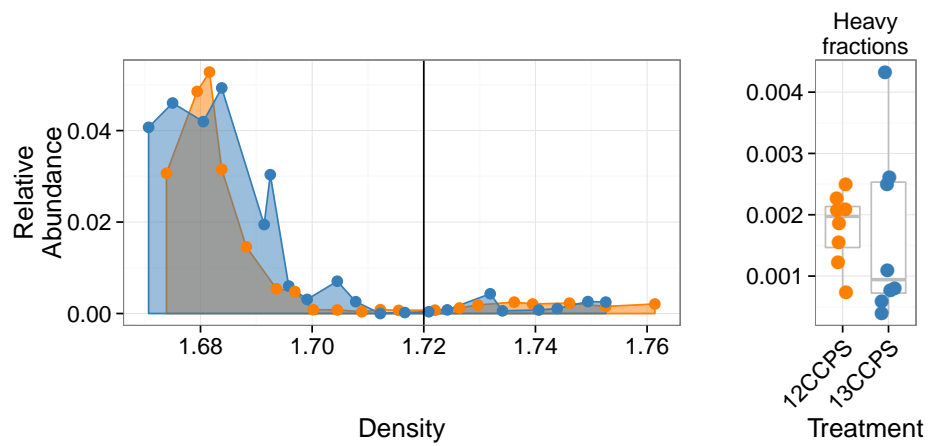


**Fig. S10.** Density profile for a single  $^{13}\text{C}$ -cellulose "non-responder" OTU in the labeled gradient, blue, and the control gradient, orange. Vertical line shows where "heavy" fractions begin as defined in our analysis. Panel at right shows relative abundance values in the heavy fractions for each gradient.

Table S1: <sup>13</sup>C-cellulose responders BLAST against Living Tree Project

OTU ID	Fold change <sup>a</sup>	Day <sup>b</sup>	Top BLAST hits	BLAST %ID	Phylum;Class;Order
OTU.100	2.66	14	<i>Pseudoxanthomonas sacheonensis</i> , <i>Pseudoxanthomonas dokdonensis</i>	100.0	Proteobacteria Gammaproteobacteria Xanthomonadales
OTU.1023	4.61	30	No hits of at least 90% identity	80.54	Verrucomicrobia Spartobacteria Chthoniobacterales
OTU.1065	5.31	14	No hits of at least 90% identity	84.55	Planctomycetes Planctomycetacia Planctomycetales
OTU.1087	4.32	14	<i>Devsia soli</i> , <i>Devsia crocina</i> , <i>Devsia riboflavina</i>	99.09	Proteobacteria Alphaproteobacteria Rhizobiales
OTU.1094	3.69	30	<i>Sporocytophaga myxococcoides</i>	99.55	Bacteroidetes Cytophagia Cytophagales
OTU.11	3.41	14	<i>Stenotrophomonas pavanii</i> , <i>Stenotrophomonas maltophilia</i> , <i>Pseudomonas geniculata</i>	99.54	Proteobacteria Gammaproteobacteria Xanthomonadales
OTU.114	2.78	14	<i>Herbaspirillum sp. SUEMI03</i> , <i>Herbaspirillum sp. SUEMI10</i> , <i>Oxalicibacterium solurbis</i> , <i>Herminiumonas fonticola</i> , <i>Oxalicibacterium horti</i>	100.0	Proteobacteria Betaproteobacteria Burkholderiales
OTU.119	3.31	14	<i>Brevundimonas alba</i>	100.0	Proteobacteria Alphaproteobacteria Caulobacterales
OTU.120	4.76	14	<i>Vampirovibrio chlorellavorus</i>	94.52	Cyanobacteria SM1D11 uncultured-bacterium
OTU.1204	4.32	30	<i>Planctomyces limnophilus</i>	91.78	Planctomycetes Planctomycetacia Planctomycetales
OTU.1312	4.07	30	<i>Paucimonas lemoignei</i>	99.54	Proteobacteria Betaproteobacteria Burkholderiales
OTU.132	2.81	14	<i>Streptomyces spp.</i>	100.0	Actinobacteria Streptomycetales Streptomycetaceae
OTU.150	4.06	14	No hits of at least 90% identity	86.76	Planctomycetes Planctomycetacia Planctomycetales
OTU.1533	3.43	30	No hits of at least 90% identity	82.27	Verrucomicrobia Spartobacteria Chthoniobacterales
OTU.154	3.24	14	<i>Pseudoxanthomonas mexicana</i> , <i>Pseudoxanthomonas japonensis</i>	100.0	Proteobacteria Gammaproteobacteria Xanthomonadales
OTU.165	3.1	14	<i>Rhizobium skieniewicense</i> , <i>Rhizobium vignae</i> , <i>Rhizobium larrymoorei</i> , <i>Rhizobium alkalisolii</i> , <i>Rhizobium galegae</i> , <i>Rhizobium huautlense</i>	100.0	Proteobacteria Alphaproteobacteria Rhizobiales
OTU.1754	4.48	14	<i>Asticcacaulis biprosthecium</i> , <i>Asticcacaulis benevestitus</i>	96.8	Proteobacteria Alphaproteobacteria Caulobacterales
OTU.185	4.37	14	No hits of at least 90% identity	85.14	Verrucomicrobia Spartobacteria Chthoniobacterales
OTU.19	2.44	14	<i>Rhizobium alamii</i> , <i>Rhizobium mesosinicum</i> , <i>Rhizobium mongolense</i> , <i>Arthrobacter viscosus</i> , <i>Rhizobium sullae</i> , <i>Rhizobium yanglingense</i> , <i>Rhizobium loessense</i>	99.54	Proteobacteria Alphaproteobacteria Rhizobiales
OTU.204	3.81	14	No hits of at least 90% identity	nan	Planctomycetes Planctomycetacia Planctomycetales

Table S1 – continued from previous page

OTU ID	Fold change	Day	Top BLAST hits	BLAST %ID	Phylum;Class;Order
OTU.2192	3.49	30	No hits of at least 90% identity	83.56	Verrucomicrobia Spartobacteria Chthoniobacterales
OTU.228	2.54	30	<i>Sorangium cellulosum</i>	98.17	Proteobacteria Deltaproteobacteria Myxococcales
OTU.241	2.66	14	No hits of at least 90% identity	87.73	Verrucomicrobia Spartobacteria Chthoniobacterales
OTU.257	2.94	14	<i>Lentzea waywayandensis</i> , <i>Lentzea flaviverrucosa</i>	100.0	Actinobacteria Pseudonocardiales Pseudonocardiaceae
OTU.266	4.54	30	No hits of at least 90% identity	83.64	Verrucomicrobia Spartobacteria Chthoniobacterales
OTU.28	2.59	14	<i>Rhizobium giardinii</i> , <i>Rhizobium tubonense</i> , <i>Rhizobium tibeticum</i> , <i>Rhizobium mesoamericanum CCGE 501</i> , <i>Rhizobium herbae</i> , <i>Rhizobium endophyticum</i>	99.54	Proteobacteria Alphaproteobacteria Rhizobiales
OTU.285	3.55	30	<i>Blastopirellula marina</i>	90.87	Planctomycetes Planctomycetacia Planctomycetales
OTU.32	2.34	3	<i>Sandaracinus amylolyticus</i>	94.98	Proteobacteria Deltaproteobacteria Myxococcales
OTU.327	2.99	14	<i>Asticcacaulis biprosthecum</i> , <i>Asticcacaulis benevestitus</i>	98.63	Proteobacteria Alphaproteobacteria Caulobacterales
OTU.351	3.54	14	<i>Pirellula staleyi DSM 6068</i>	91.86	Planctomycetes Planctomycetacia Planctomycetales
OTU.3594	3.83	30	<i>Chondromyces robustus</i>	90.41	Proteobacteria Deltaproteobacteria Myxococcales
OTU.3775	3.88	14	<i>Devosia glacialis</i> , <i>Devosia chinhatensis</i> , <i>Devosia geojensis</i> , <i>Devosia yakushimensis</i>	98.63	Proteobacteria Alphaproteobacteria Rhizobiales
OTU.429	3.7	30	<i>Devosia limi</i> , <i>Devosia psychrophila</i>	97.72	Proteobacteria Alphaproteobacteria Rhizobiales
OTU.4322	4.19	14	No hits of at least 90% identity	89.14	Chloroflexi Herpetosiphonales Herpetosiphonaceae
OTU.442	3.05	30	<i>Chondromyces robustus</i>	92.24	Proteobacteria Deltaproteobacteria Myxococcales
OTU.465	3.79	30	<i>Ohtaekwangia kribbensis</i>	92.73	Bacteroidetes Cytophagia Cytophagales
OTU.473	3.58	14	<i>Pirellula staleyi DSM 6068</i>	90.91	Planctomycetes Planctomycetacia Planctomycetales
OTU.484	4.92	14	No hits of at least 90% identity	89.09	Planctomycetes Planctomycetacia Planctomycetales
OTU.5	2.69	14	<i>Delftia tsuruhatensis</i> , <i>Delftia lacustris</i>	100.0	Proteobacteria Betaproteobacteria Burkholderiales
OTU.518	4.8	14	<i>Hydrogenophaga intermedia</i>	100.0	Proteobacteria Betaproteobacteria Burkholderiales
OTU.5190	3.6	30	No hits of at least 90% identity	88.13	Chloroflexi Herpetosiphonales Herpetosiphonaceae
OTU.541	4.49	30	No hits of at least 90% identity	84.23	Verrucomicrobia Spartobacteria Chthoniobacterales
OTU.5539	4.01	14	<i>Devosia subaequoris</i>	98.17	Proteobacteria Alphaproteobacteria Rhizobiales

Table S1 – continued from previous page

OTU ID	Fold change	Day	Top BLAST hits	BLAST %ID	Phylum;Class;Order
OTU.573	3.03	30	<i>Adhaeribacter aerophilus</i>	92.76	<i>Bacteroidetes Cytophagia Cytophagales</i>
OTU.6	3.62	7	<i>Cellvibrio fulvus</i>	100.0	<i>Proteobacteria Gammaproteobacteria Pseudomonadales</i>
OTU.600	3.48	30	No hits of at least 90% identity	80.37	<i>Planctomycetes Planctomycetacia Planctomycetales</i>
OTU.6062	4.83	30	<i>Dokdonella sp. DC-3, Luteibacter rhizovicinus</i>	97.26	<i>Proteobacteria Gammaproteobacteria Xanthomonadales</i>
OTU.627	4.43	14	<i>Verrucomicrobiaceae bacterium DC2a-G7</i>	100.0	<i>Verrucomicrobia Verrucomicrobiae Verrucomicrobiales</i>
OTU.633	3.84	30	No hits of at least 90% identity	89.5	<i>Proteobacteria Deltaproteobacteria Myxococcales</i>
OTU.638	4.0	30	<i>Luteolibacter sp. CCTCC AB 2010415, Luteolibacter algae</i>	93.61	<i>Verrucomicrobia Verrucomicrobiae Verrucomicrobiales</i>
OTU.64	4.31	14	No hits of at least 90% identity	89.5	<i>Chloroflexi Herpetosiphonales Herpetosiphonaceae</i>
OTU.663	3.63	30	<i>Pirellula staleyi DSM 6068</i>	90.87	<i>Planctomycetes Planctomycetacia Planctomycetales</i>
OTU.669	3.34	30	<i>Ohtaekwangia koreensis</i>	92.69	<i>Bacteroidetes Cytophagia Cytophagales</i>
OTU.670	2.87	30	<i>Adhaeribacter aerophilus</i>	91.78	<i>Bacteroidetes Cytophagia Cytophagales</i>
OTU.766	3.21	14	<i>Devosia insulae</i>	99.54	<i>Proteobacteria Alphaproteobacteria Rhizobiales</i>
OTU.83	5.61	14	<i>Luteolibacter sp. CCTCC AB 2010415</i>	97.72	<i>Verrucomicrobia Verrucomicrobiae Verrucomicrobiales</i>
OTU.862	5.87	14	<i>Allokutzneria albata</i>	100.0	<i>Actinobacteria Pseudonocardiales Pseudonocardiaceae</i>
OTU.899	2.28	30	<i>Enhygromyxa salina</i>	97.72	<i>Proteobacteria Deltaproteobacteria Myxococcales</i>
OTU.90	2.94	14	<i>Sphingopyxis panaciterrae, Sphingopyxis chilensis, Sphingopyxis sp. BZ30, Sphingomonas sp.</i>	100.0	<i>Proteobacteria Alphaproteobacteria Sphingomonadales</i>
OTU.900	4.87	14	<i>Brevundimonas vesicularis, Brevundimonas nasdae</i>	100.0	<i>Proteobacteria Alphaproteobacteria Caulobacterales</i>
OTU.971	3.68	30	No hits of at least 90% identity	78.57	<i>Chloroflexi Anaerolineae Anaerolineales</i>
OTU.98	3.68	14	No hits of at least 90% identity	88.18	<i>Chloroflexi Herpetosiphonales Herpetosiphonaceae</i>
OTU.982	4.47	14	<i>Devosia neptuniae</i>	100.0	<i>Proteobacteria Alphaproteobacteria Rhizobiales</i>

<sup>a</sup> Maximum observed  $\log_2$  of fold change.<sup>b</sup> Day of maximum fold change.

Table S2:  $^{13}\text{C}$ -xylose responders BLAST against Living Tree Project

OTU ID	Fold change <sup>a</sup>	Day <sup>b</sup>	Top BLAST hits	BLAST %ID	Phylum;Class;Order
OTU.1040	4.78	1	<i>Paenibacillus daejeonensis</i>	100.0	<i>Firmicutes Bacilli Bacillales</i>
OTU.1069	3.85	1	<i>Paenibacillus terrigena</i>	100.0	<i>Firmicutes Bacilli Bacillales</i>
OTU.107	2.25	3	<i>Flavobacterium sp. 15C3</i> , <i>Flavobacterium banpakuense</i>	99.54	<i>Bacteroidetes Flavobacteria Flavobacteriales</i>
OTU.11	5.25	7	<i>Stenotrophomonas pavanii</i> , <i>Stenotrophomonas maltophilia</i> , <i>Pseudomonas geniculata</i>	99.54	<i>Proteobacteria Gammaproteobacteria Xanthomonadales</i>
OTU.131	3.07	3	<i>Flavobacterium fluvii</i> , <i>Flavobacterium bacterium HMD1033</i> , <i>Flavobacterium sp. HMD1001</i>	100.0	<i>Bacteroidetes Flavobacteria Flavobacteriales</i>
OTU.14	3.92	3	<i>Flavobacterium oncorhynchi</i> , <i>Flavobacterium glycines</i> , <i>Flavobacterium succinicans</i>	99.09	<i>Bacteroidetes Flavobacteria Flavobacteriales</i>
OTU.150	3.08	14	No hits of at least 90% identity	86.76	<i>Planctomycetes Planctomycetacia Planctomycetales</i>
OTU.159	3.16	3	<i>Flavobacterium hibernum</i>	98.17	<i>Bacteroidetes Flavobacteria Flavobacteriales</i>
OTU.165	2.38	3	<i>Rhizobium skieniewicense</i> , <i>Rhizobium vignae</i> , <i>Rhizobium larrymoorei</i> , <i>Rhizobium alkalisolii</i> , <i>Rhizobium galegae</i> , <i>Rhizobium huautlense</i>	100.0	<i>Proteobacteria Alphaproteobacteria Rhizobiales</i>
OTU.183	3.31	3	No hits of at least 90% identity	89.5	<i>Bacteroidetes Sphingobacteriia Sphingobacteriales</i>
OTU.19	2.14	7	<i>Rhizobium alamii</i> , <i>Rhizobium mesosinicum</i> , <i>Rhizobium mongolense</i> , <i>Arthrobacter viscosus</i> , <i>Rhizobium sullae</i> , <i>Rhizobium yanglingense</i> , <i>Rhizobium loessense</i>	99.54	<i>Proteobacteria Alphaproteobacteria Rhizobiales</i>
OTU.2040	2.91	1	<i>Paenibacillus pectinilyticus</i>	100.0	<i>Firmicutes Bacilli Bacillales</i>
OTU.22	2.8	7	<i>Paracoccus sp. NB88</i>	99.09	<i>Proteobacteria Alphaproteobacteria Rhodobacterales</i>
OTU.2379	3.1	3	<i>Flavobacterium pectinovorum</i> , <i>Flavobacterium sp. CS100</i>	97.72	<i>Bacteroidetes Flavobacteria Flavobacteriales</i>
OTU.24	2.81	7	<i>Cellulomonas aerilata</i> , <i>Cellulomonas humilata</i> , <i>Cellulomonas terrae</i> , <i>Cellulomonas soli</i> , <i>Cellulomonas xylinilytica</i>	100.0	<i>Actinobacteria Micrococcales Cellulomonadaceae</i>
OTU.241	3.38	3	No hits of at least 90% identity	87.73	<i>Verrucomicrobia Spartobacteria Chthoniobacterales</i>
OTU.244	3.08	7	<i>Cellulosimicrobium funkei</i> , <i>Cellulosimicrobium terreum</i>	100.0	<i>Actinobacteria Micrococcales Promicromonosporaceae</i>
OTU.252	3.34	7	<i>Promicromonospora thailandica</i>	100.0	<i>Actinobacteria Micrococcales Promicromonosporaceae</i>
OTU.267	4.97	1	<i>Paenibacillus pabuli</i> , <i>Paenibacillus tundrae</i> , <i>Paenibacillus taichungensis</i> , <i>Paenibacillus xylohexedens</i> , <i>Paenibacillus xylinilyticus</i>	100.0	<i>Firmicutes Bacilli Bacillales</i>
OTU.277	3.52	3	<i>Solibius ginsengiterrae</i>	95.43	<i>Bacteroidetes Sphingobacteriia Sphingobacteriales</i>

Table S2 – continued from previous page

OTU ID	Fold change	Day	Top BLAST hits	BLAST %ID	Phylum;Class;Order
OTU.290	3.59	1	<i>Pantoea spp.</i> , <i>Klugvera spp.</i> , <i>Klebsiella spp.</i> , <i>Erwinia spp.</i> , <i>Enterobacter spp.</i> , <i>Buttiauxella spp.</i>	100.0	Proteobacteria Gammaproteobacteria Enterobacterales
OTU.3	2.61	1	[ <i>Brevibacterium</i> ] <i>frigoritolerans</i> , <i>Bacillus sp. LMG 20238</i> , <i>Bacillus coahuilensis m4-4</i> , <i>Bacillus simplex</i>	100.0	Firmicutes Bacilli Bacillales
OTU.319	3.98	1	<i>Paenibacillus xinjiangensis</i>	97.25	Firmicutes Bacilli Bacillales
OTU.32	3.0	3	<i>Sandaracinus amyloyticus</i>	94.98	Proteobacteria Deltaproteobacteria Myxococcales
OTU.335	2.53	1	<i>Paenibacillus thailandensis</i>	98.17	Firmicutes Bacilli Bacillales
OTU.346	3.44	3	<i>Pseudoduganella violaceinigra</i>	99.54	Proteobacteria Betaproteobacteria Burkholderiales
OTU.3507	2.36	1	<i>Bacillus spp.</i>	98.63	Firmicutes Bacilli Bacillales
OTU.3540	2.52	3	<i>Flavobacterium terrigena</i>	99.54	Bacteroidetes Flavobacteria Flavobacterales
OTU.360	2.98	3	<i>Flavisolibacter ginsengisoli</i>	95.0	Bacteroidetes Sphingobacteriia Sphingobacterales
OTU.369	5.05	1	<i>Paenibacillus sp. D75</i> , <i>Paenibacillus glycansilyticus</i>	100.0	Firmicutes Bacilli Bacillales
OTU.37	2.68	7	<i>Phycicola gilvus</i> , <i>Microterricola viridarii</i> , <i>Frigeribacterium faeni</i> , <i>Frondihabitans sp. RS-15</i> , <i>Frondihabitans australicus</i>	100.0	Actinobacteria Micrococcales Microbacteriaceae
OTU.394	4.06	1	<i>Paenibacillus pocheonensis</i>	100.0	Firmicutes Bacilli Bacillales
OTU.4	2.84	7	<i>Agromyces ramosus</i>	100.0	Actinobacteria Micrococcales Microbacteriaceae
OTU.4446	3.49	7	<i>Catenuloplanes niger</i> , <i>Catenuloplanes castaneus</i> , <i>Catenuloplanes atrovinosus</i> , <i>Catenuloplanes crispus</i> , <i>Catenuloplanes nepalensis</i> , <i>Catenuloplanes japonicus</i>	97.72	Actinobacteria Frankiales Nakamurellaceae
OTU.4743	2.24	1	<i>Lysinibacillus fusiformis</i> , <i>Lysinibacillus sphaericus</i>	99.09	Firmicutes Bacilli Bacillales
OTU.48	2.99	1	<i>Aeromonas spp.</i>	100.0	Proteobacteria Gammaproteobacteria aaa34a10
OTU.5	3.69	7	<i>Delftia tsuruhatensis</i> , <i>Delftia lacustris</i>	100.0	Proteobacteria Betaproteobacteria Burkholderiales
OTU.5284	3.56	7	<i>Isopotericola nanjingensis</i> , <i>Isopotericola hypogaeus</i> , <i>Isopotericola variabilis</i>	98.63	Actinobacteria Micrococcales Promicromonosporaceae
OTU.5603	3.96	1	<i>Paenibacillus uliginis</i>	100.0	Firmicutes Bacilli Bacillales
OTU.57	4.39	1	<i>Paenibacillus castaneae</i>	98.62	Firmicutes Bacilli Bacillales
OTU.5906	3.16	3	<i>Terrimonas sp. M-8</i>	96.8	Bacteroidetes Sphingobacteriia Sphingobacterales
OTU.6	3.24	3	<i>Cellvibrio fulvus</i>	100.0	Proteobacteria Gammaproteobacteria Pseudomonadales
OTU.62	2.57	7	<i>Nakamurella flava</i>	100.0	Actinobacteria Frankiales Nakamurellaceae

Table S2 – continued from previous page

OTU ID	Fold change	Day	Top BLAST hits	BLAST %ID	Phylum;Class;Order
OTU.6203	3.32	3	<i>Flavobacterium granuli</i> , <i>Flavobacterium glaciei</i>	100.0	<i>Bacteroidetes Flavobacteria Flavobacteriales</i>
OTU.68	3.74	7	<i>Shigella flexneri</i> , <i>Escherichia fergusonii</i> , <i>Escherichia coli</i> , <i>Shigella sonnei</i>	100.0	<i>Proteobacteria Gammaproteobacteria Enterobacteriales</i>
OTU.760	2.89	3	<i>Dyadobacter hamtensis</i>	98.63	<i>Bacteroidetes Cytophagia Cytophagales</i>
OTU.8	2.26	1	<i>Bacillus niaci</i>	100.0	<i>Firmicutes Bacilli Bacillales</i>
OTU.843	3.62	1	<i>Paenibacillus agaragedens</i>	100.0	<i>Firmicutes Bacilli Bacillales</i>
OTU.9	2.04	1	<i>Bacillus megaterium</i> , <i>Bacillus flexus</i>	100.0	<i>Firmicutes Bacilli Bacillales</i>

<sup>a</sup> Maximum observed  $\log_2$  of fold change.<sup>b</sup> Day of maximum fold change.